Title:

Evaluation of at-home methods for N95 filtering facepiece respirator decontamination

One sentence summary:

Survey of at-home methods for N95 respirator decontamination using heat and evaluation of their effects on N95 respirator integrity.

Authors:

Tiffany X. Chen[1]*, Ana Pinharanda[2]*, Keiko Yasuma-Mitobe[3], Elaine Lee[4], Natalie A. Steinemann[1], Jaeseung Hahn[5], Lydia Wu[4], Stavros Fanourakis[6], Darcy S. Peterka[1]†, Elizabeth M.C. Hillman[1,5,7]†

* These authors contributed equally to this work

† Corresponding authors. Emails: eh2245@columbia.edu, dp2403@columbia.edu

Affiliations:

[1]Mortimer B. Zuckerman Mind Brain Behavior Institute, New York, NY, 10027, USA

[2]Department of Biological Sciences, Columbia University, New York, NY 10027, USA

[3]Department of Microbiology and Immunology, Columbia University, New York, NY 10032, USA

[4]Columbia College, Columbia University, New York, NY 10032, USA

[5]Department of Biomedical Engineering, Columbia University, New York, NY 10027, USA

[6]Environmental Health and Safety, Columbia University, New York, NY 10032, USA

[7]Department of Radiology, Columbia University, New York, NY 10027, USA

Abstract:

Shortages in N95 filtering facepiece respirators (FFRs) are significant as FFRs are essential for the protection of healthcare professionals and other high-risk groups against Coronavirus Disease of 2019 (COVID-19), a disease caused by severe acute respiratory syndrome coronavirus 2. In response to these shortages during the ongoing COVID-19 pandemic, the Food and Drug Administration issued an Emergency Use Authorization (EUA) permitting FFR decontamination and reuse. However, although industrial decontamination services are available at some large institutions, FFR decontamination is not widely available.

Effective FFR decontamination must 1) deactivate the virus; 2) preserve FFR integrity, specifically fit and filtering capability; and 3) be non-toxic and safe. Here we identify and compare at-home methods for heat-based FFR decontamination that meet these requirements, but utilize common household appliances. Our results identify viable protocols for simple and accessible FFR decontamination, while also highlighting methods that may jeopardize FFR integrity and should be avoided.

Main text:

INTRODUCTION

Coronavirus Disease of 2019 (COVID-19), caused by severe acute respiratory syndrome coronavirus 2 (SARS-CoV-2), is thought to be transmitted predominantly through exposure to short-range droplets and aerosols [1]. To protect against infectious airborne particles, possibly including sub-micrometer aerosols carrying SARS-CoV-2 [2], filtering facepiece respirators (FFRs) such as the N95 [3] are recommended by the United States Center for Disease Control and Prevention (CDC) as the PPE

standard for healthcare professionals [4]. With appropriate donning and doffing procedures, combined with proper fit, N95 FFRs can effectively limit cross-contamination and the transmission of COVID-19 [5].

Limiting disease transmission is one of the primary means of controlling the COVID-19 outbreak [6]. However, the global increase in demand for personal protective equipment (PPE) during the ongoing COVID-19 pandemic has led to an international shortage of high-performance FFRs [3]. Under conventional standards, N95 FFRs are intended to be disposable and are not approved for reuse. However, the rapid increase in hospitalizations, combined with large public demand for PPE, resulted in severe shortages and significant price inflation of N95 FFRs. This led the Food and Drug Administration (FDA) to issue an emergency use authorization for N95 FFR reuse and decontamination during the COVID-19 pandemic [7]. Several different approaches can be used to decontaminate FFRs, as defined by the FDA to be a minimum of a 3-log (i.e., 99.9%) reduction in SARS-CoV-2 viral activity [8]. In addition to inactivating the virus, decontamination strategies for N95 FFR reuse must maintain overall mask integrity, as measured by fit (ability to form a tight seal) and filtration (ability to limit penetration of particulates) [9].

Some methods of decontamination have been shown to satisfy these criteria. For example, ultraviolet (UV) germicidal irradiation (radiation-based); hydrogen peroxide vapor (HPV) (chemical-based); and heat-humidity treatments [10], have all been used successfully. Unfortunately, these procedures can be difficult to implement reliably at a large scale, and/or present safety risks at a small scale, especially in resource-limited environments, outside large hospitals or research settings. HPV, for example, is a

severe irritant that can be hazardous to the lungs and eyes. Most UV-C light sources have spectral variation, including wavelengths that can damage the skin or eyes, and proper decontamination by UV-C light requires every surface to receive a sufficient dose of radiant energy, which is hard to ensure for masks due to their three-dimensional shape and metal inserts [11].

Another significant obstacle is that methods that provide sterilization, the complete elimination of all forms of microbial life, using heat (e.g., autoclaving) are highly likely to damage mask integrity. As a result, existing FFR decontamination methods, even though effective against SARS-CoV-2, do not typically remove all other forms of pathogens and contaminants. This constraint necessitates returning decontaminated masks to the original user, a major logistical challenge on an institutional scale, particularly during a healthcare crisis. Therefore, establishing safe and economical decontamination methods for FFR reuse, that could be implemented in a personal, household or resource-limited setting, is both necessary and urgent, considering the current global strain on the supply of N95 FFRs and the vast number of individuals vulnerable to COVID-19 and other respirable infectious agents worldwide.

In this study, we recognized the potential of widely available, commercial household heat-generating appliances to be used for FFR decontamination. We performed quantitative testing of a series of appliances and decontamination methods, evaluating both their ability to reliably establish and maintain decontamination conditions, and the effects of repeated treatments on mask fit and material filtration performance. We identify rice cookers with thermostatically-controlled warming functions as being the best of our tested heat-treatment methods at achieving decontamination conditions for

N95 FFRs reuse by retaining FFR fit and filtration integrity for up to five repeated treatments. We also confirm that boiling FFRs is damaging to FFR fit.

RESULTS

Establishing decontamination parameters through literature review

Based on a review of previous studies that successfully used heat to deactivate enveloped viruses, we identified parameters that were likely to inactivate SARS-CoV-2 within FFR fabric using heat, while also preserving the fit and filtering properties of the mask. As a result of the COVID-19 response, extensive non-regulatory agency (e.g., National Institute for Occupational Safety and Health (NIOSH), CDC) testing and review of N95 decontamination strategies have been done [12]. Table 1 summarizes 1) temperature, humidity, exposure times and substrates that achieve viral inactivation; and 2) how these different conditions were found to affect FFR fit and filtration.

Strain	Medium	Model	Method	Temp (ºC)	Humidity (%RH)	Time (min)	log reduction in virus	Filtration test passed after # treatments	Fit test passed after # treatments	Source
SARS-CoV-2	N/A	3M 1860S, 8110S, 8210S, 9105S	Dry heat	70	50	60	> 3	10	5	[13]
		AO safety N9504C				30	Insufficient	N/A	N/A	
						60	> 3.3	N/A	N/A	
	Bovine serum albumin, tryptone, mucin	3M 1860, 3M 1870, 3M Vflex 1804, AO Safety 1054	Steam	121	N/A	15	> 4.6-5.6	1-10	4	[14]
	DMEM	AOSafety N9504C	Dry heat	70	N/A	60	> 3	2	N/A	[15]
	DMEM	3M 1860	Dry heat	72	1	30	Insufficient	N/A	N/A	[16]
				82	25					

Murine coronavirus MHV				72	25		> 3.5			
		3M 8210	Humid heat	75	90	30	> 6	N/A	10	[17]
H5N1	Aerosolized allantonic fluid	3M 1860S, 3M 1870	Humid heat	65	N/A	30	> 4.62-4.65	N/A	N/A	[18]

Table 1. Effect of heat and humidity on enveloped viruses on N95 FFRs. Log viral reduction >3 is sufficient to consider the virus inactivated. N/A: Not Applicable, the parameter was not tested. DMEM refers to Dulbecco's Modified Eagle Medium.

In conjunction, these studies indicate that sustaining a temperature of 70-85°C for 30 minutes at 50% humidity [17,19] or 60 minutes (with dry heat [15]) should be sufficient to inactivate SARS-CoV-2. Based on prior studies [10], we hypothesized that both of these conditions should preserve fit and filtration efficiency of FFRs for up to five rounds of treatment, in line with the CDC's recommendation of a maximum of five donning and doffing cycles for FFRs [10]. Additionally, treatment with steam autoclaves or immersion boiling should inactivate SARS-CoV-2 from FFRs, but previous studies indicated that these types of treatments may reduce FFR filtration efficiency and impact fit after as few as one round of treatment [14,20].

Identifying home appliances capable of accurately attaining decontamination conditions

A wide range of commercial heat-generating appliances, including microwaves, rice cookers, sous vide machines, tumble driers, hair dryers, and ovens, were considered for achieving FFR-compatible heat conditions of 70°C for one hour. Appliances with minimum temperatures nominally above 70ºC or maximum temperatures nominally below 70ºC were first excluded. For example, standard gas ovens cannot be programmed to maintain temperatures lower than 76.7°C [21] and commercial tumble dryers and hair dryers do not exceed 60ºC during operation at the hottest setting [22]. Appliances that posed a

potential safety risk to the user were also deemed unsuitable. Microwave-generated heat may cause FFRs with metallic components, such as the nosepiece, to spark or the plastic from the straps to melt [23,24].

Based on these temperature and safety criteria, we selected rice cookers and sous vide machines for further evaluation [25,26]. Although many types of rice cookers with varying quality and accuracy exist, only a subset can maintain relatively precise temperatures around our target temperature of 70-85°C through a *Keep Warm* setting. Sous vide machines, with basic components that include a heating element, temperature feedback circuit, and water circulator, are the basis for a popular method of cooking which involves encasing food inside water-tight plastic bags and heating it in temperature-controlled water. The sous-vide machine is dipped into the water, circulating it and establishing and precisely maintaining the desired cooking temperature (over a range including our desired 70-85°C condition).

Two types of rice cookers with *Keep Warm* settings were selected for testing: 1) the Cuckoo (CR-0655F, retail ~$110), and 2) the Aroma (ARC-743-1NGB, retail ~$20). We also tested an AuAg Immersion Circulator sous vide machine (A808, 950 W, retail ~$50).

Basic device performance assessment

Initial testing was performed to confirm whether each device could reach and maintain a target temperature of 70°C for one hour. A one hour treatment time was chosen since none of the selected devices were expected to reliably provide and maintain the 50% humidity level required for a 30-minute treatment. For both rice cookers, a temperature sensor (Inkbird Thermometer IBS-TH1) was

placed in an elevated plastic tub containing 120 ml of water within the inner pot and heated using the *Keep Warm* setting. For the sous vide machine, a temperature sensor (MeatStick Wireless Thermometer 4335995327) was immersed in a 20.5 x 15.5 x 12 cm^3 polystyrene box with 3.2 L of water and warmed using a sous-vide temperature setting of 70ºC. Temperature was recorded during initial heating and then for one hour after each appliance's temperature had stabilized. The total process time, including time to reach the target temperature, were also recorded (Table 2, Fig S1).

Type	Appliance	Temperature (°C)		
		Min	Mean	Max
Rice cooker	Cuckoo (CR-0655F)	69.7	71.7	72.2
	Aroma (ARC-743-1NGB)	63.5	67.5	69.5
Sous vide	AuAg Immersion Circulator (A808, 950 W)	68.5	70.1	70.5

Table 2. Temperature maintained after initial heating period in the appliances tested. The Cuckoo (CR-0655F) *Keep Warm* setting maintained an average temperature of 71.7°C (-2.0°C /+0.5°C). The sous vide AuAg Immersion Circulator (A808, 950 W) has an average temperature of 69.8°C (-1.6°C /+0.4°C). The Aroma (ARC-743-1NGB) *Keep Warm* setting reached an average temperature of 67.5°C (-4.0°C /+2.0°C).

The *Keep Warm* setting of the Cuckoo rice cooker and the AuAg Immersion Circulator sous vide machine were confirmed to have precise temperature control. The time to reach the target temperature of 70ºC was 23.3 ± 7.8 minutes for the Cuckoo rice cooker and 14.3 ± 1.5 minutes for the sous vide machine (Fig S1) [10,20]. With a process temperature of 67.5ºC ± 7.8 ºC across the hour-long treatment, the *Keep Warm* setting of the Aroma rice cooker did not allow for precise temperature control. As it was impossible to maintain a stable temperature within the required range, the Aroma rice cooker was excluded from all subsequent tests. This result suggests that, even among rice cookers with *Keep Warm*

functions, not all may be suitable for FFR decontamination, and users should consult appliance manuals and specifications to confirm the device's ability to maintain the specified temperature range.

Evaluating the effects of appliance-based heat treatment on quantitative FFR fit

Based on the temperature measurements, we decided to test and compare the effects of three different decontamination protocols on mask fit and function: 1) boiling at 100ºC for 10 minutes, 2) maintaining 70ºC for 60 minutes using the Cuckoo rice cooker and 3) maintaining 70ºC for 60 minutes using the sous vide machine. Boiling was included as it is simple to perform at home, but was expected to impair FFR function [9,14] (Fig 1).

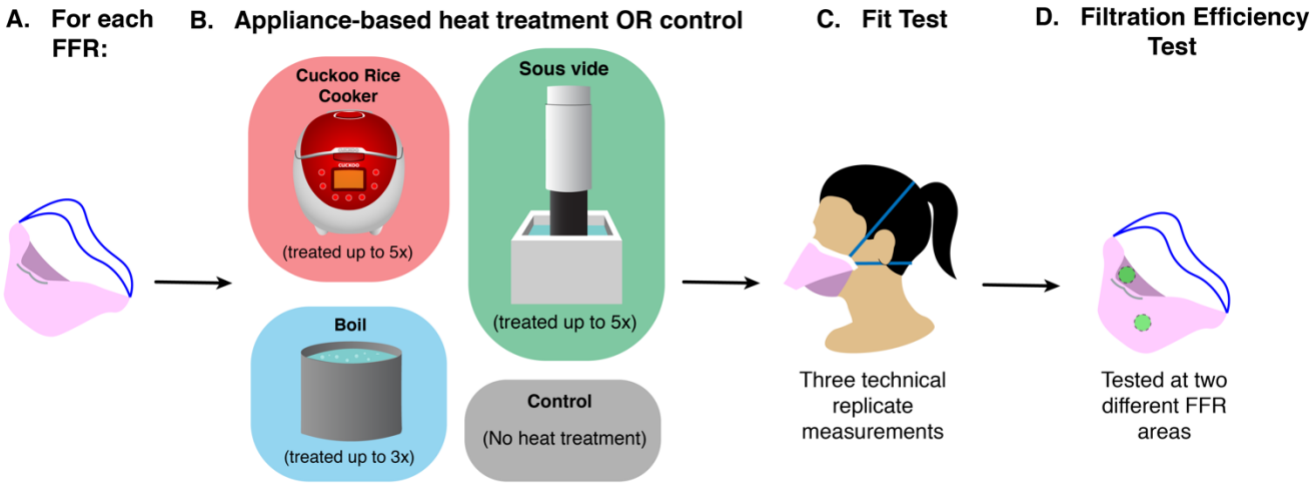

Fig 1. Experimental workflow for Halyard Fluidshield 3 (TC-84A-7521) FFRs. (A) Each FFR was blind assigned to either **(B)** *x* round(s) of appliance-based heat treatment OR to a control group. We tested three appliance-based heat treatment methods: Cuckoo rice cooker, sous vide machine and boiling. Boiled FFRs were treated up to three times. FFRs heated with sous vide machine and Cuckoo rice cooker were treated up to five times. Control FFRs were not exposed to any treatment. **(C)** Treatment-exposed and control FFRs were fit tested using the built-in N95 setting of a TSI PortaCount Pro+ Respirator Fit Tester 8038. Three technical replicate measurements were taken for each FFR and overall Fit Factors (Fig 2) and fit values for the different testing categories (Fig 3) were recorded. **(D)** The effect of appliance-based heat treatment on FFR filtration performance was evaluated for treatment and

control FFRs using a modified version of the standard NIOSH test (Fig 4). Filtration efficiency was tested on two different FFR areas. For the Uniair San Huei SH3500 (TC-84A-4313) model, FFRs were only exposed to heat using the Cuckoo rice cooker and the sous vide machine. They were treated up to three times. Fit was estimated for both treatment and control FFRs as it is described in (C), the masks were not tested for filtration performance.

FFRs assigned to be heated by the rice cooker were placed in breathable paper bags during the treatment in order to reproduce how a home user would be advised to handle contaminated FFRs (Fig 2, bottom center picture) [10]. For heat treatment with the sous vide machine, FFRs were sealed securely in a polypropylene plastic bag (double protection Ziploc© Freezer Bags) before being placed in water. In order to completely submerge the FFR within water, two 140 g weights were placed on top of the plastic bag (Fig 2, bottom right picture). For boiled FFRs, as described in a previous study [9], the N95 mask material was directly immersed in the water while most of the elastic components were kept out of the water to prevent altering the elasticity (Fig 2, bottom left picture). For all three conditions, extra care was taken to ensure that the masks were positioned flat for the duration of the treatment in order to avoid deforming the mask.

Experiments were performed using two models of donated FFRs: the Halyard Fluidshield 3 (TC-84A-7521) (Fig 2, top) and the Uniair San Huei SH3500 (TC-84A-4313) (Fig S2). Care was taken to minimize the total number of masks used in these experiments considering that this research was conducted during the pandemic when PPE supplies were limited. Individual FFRs underwent one to five rounds of heat treatment followed by quantitative fit testing, and material filtration assessment in comparison to an untreated control (IRB reference AAAT5503) (Fig 1, Fig S2 and Supplemental Methods for full details of treatments and fit testing protocols).

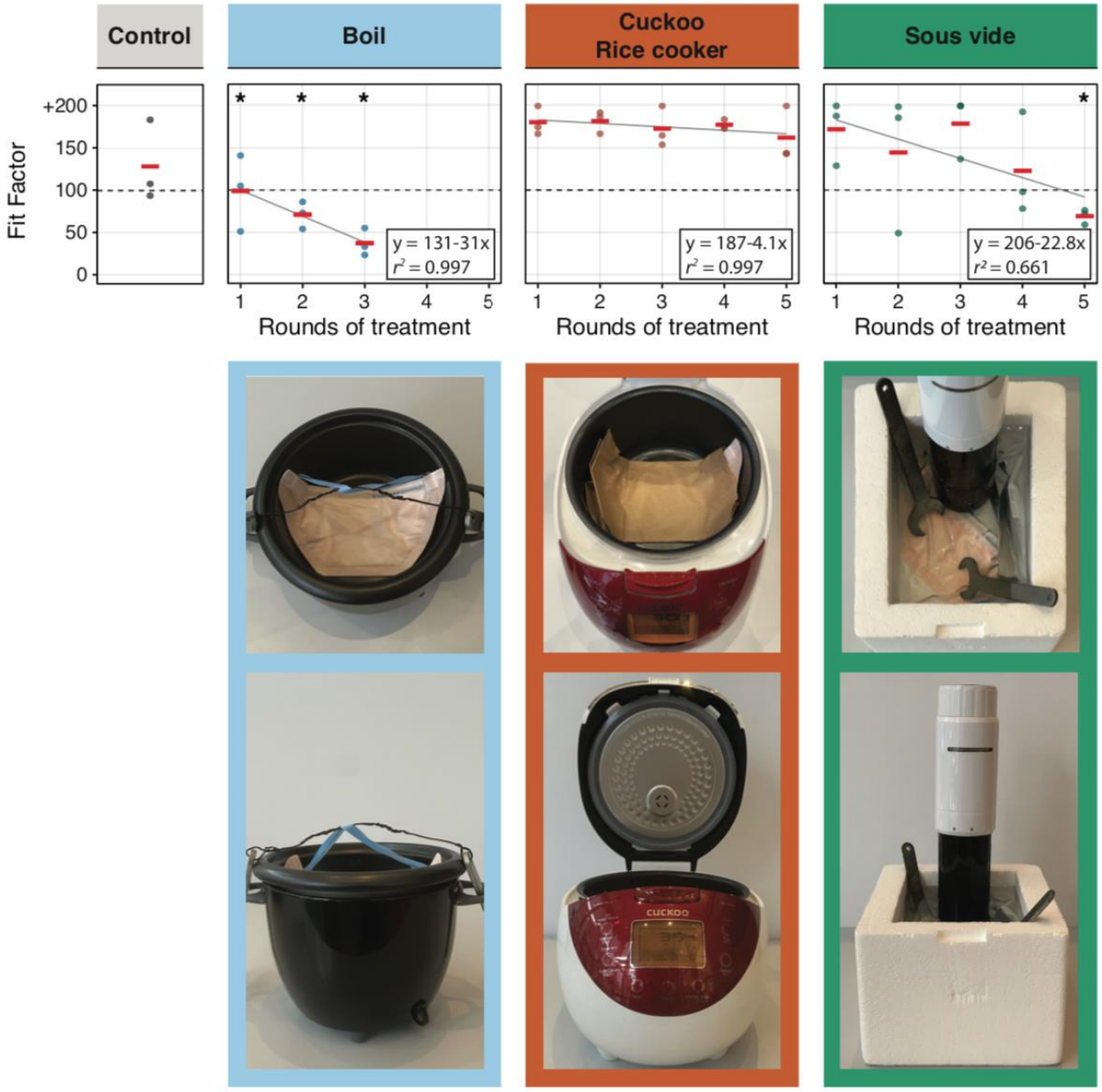

Fig 2. Average Halyard Fluidshield 3 FFR fit factor. After exposing FFRs to different methods and repetitions of heat-treatment, the fit factor was estimated with the PortaCountPro+. The fit factor was estimated three times for each FFR (smaller dots) and average fit factor is reported to the nearest integer (red bar). The control FFR was not subjected to any rounds of heat treatment. Grey regression line is overlaid for each treatment method ($y \sim mx + b$). Analysis of variance p-values is shown when there is significant variation in means among treatment group and control. Significance (*) $p < 0.05$. Photographs of the heat generation appliances shown in the panel below their respective fit factor profile.

As shown in Fig 2 (top), exposing Halyard Fluidshield 3 FFRs to 70°C of dry heat for 60 minutes in the Cuckoo rice cooker up to five times did not decrease their fit quality (no significant difference among test group and the control FFR; $p > 0.05$). Halyard Fluidshield 3 FFRs that were treated with the sous vide machine showed a significant decrease in fit quality, and failed fit testing after four rounds of treatment ($p < 0.01$). Halyard Fluidshield 3 FFRs boiled for ten minutes failed fit testing after the second round ($p < 0.01$) (Fig 2 and Table S1). We conclude from these results that, out of the three tested methods, the Cuckoo rice cooker, and by extension, dry heat, is best at preserving Halyard Fluidshield 3 FFR fit.

Fig S3 shows equivalent analyses for the Uniair FFR model. However, overall fit quality of this FFR on our testers was found to be poor, and even the control FFR failed two out of three technical replicate fit test measurements (Fig S3, Fig S4, Table S2 and Table S3). Based on our recorded poor fit performance and the lack of trends in fit quality with treatment conditions (Fig S4), we cannot meaningfully draw conclusions on how the number of treatment repetitions affect the Uniair FFR fit. These results underscore the importance of performing regular quantitative fit testing of specific PPE to specific subjects to ensure proper FFR fit under a respiratory protection plan [27]. The conclusions of this paper regarding FFR fit and filtration efficacy after treatment thus pertain primarily to the Halyard Fluidshield 3 (TC-84A-7521). It is, however, possible that trends in fit following heat-treatment holds for similarly manufactured FFRs.

Comparison of individual fit test categories gives insights into how to improve fit

Quantitative fit testing of FFRs involves a series of different test conditions for a specific wearer (*normal breathing*, *deep breathing*, *head side to side*, *head up and down*, *talking*, *bending over*, and *normal breathing*). These results are often only examined using the overall fit factor, a geometric mean of the individual categories. However, more detailed analysis (Fig 3) of results for each part of the test can provide valuable insights. For example, while FFRs exposed to 70°C in the Cuckoo rice cooker passed

fit testing after five rounds of treatment, and sous vide machine FFRs passed after four rounds of treatment, they did not score equally in all the test's categories.

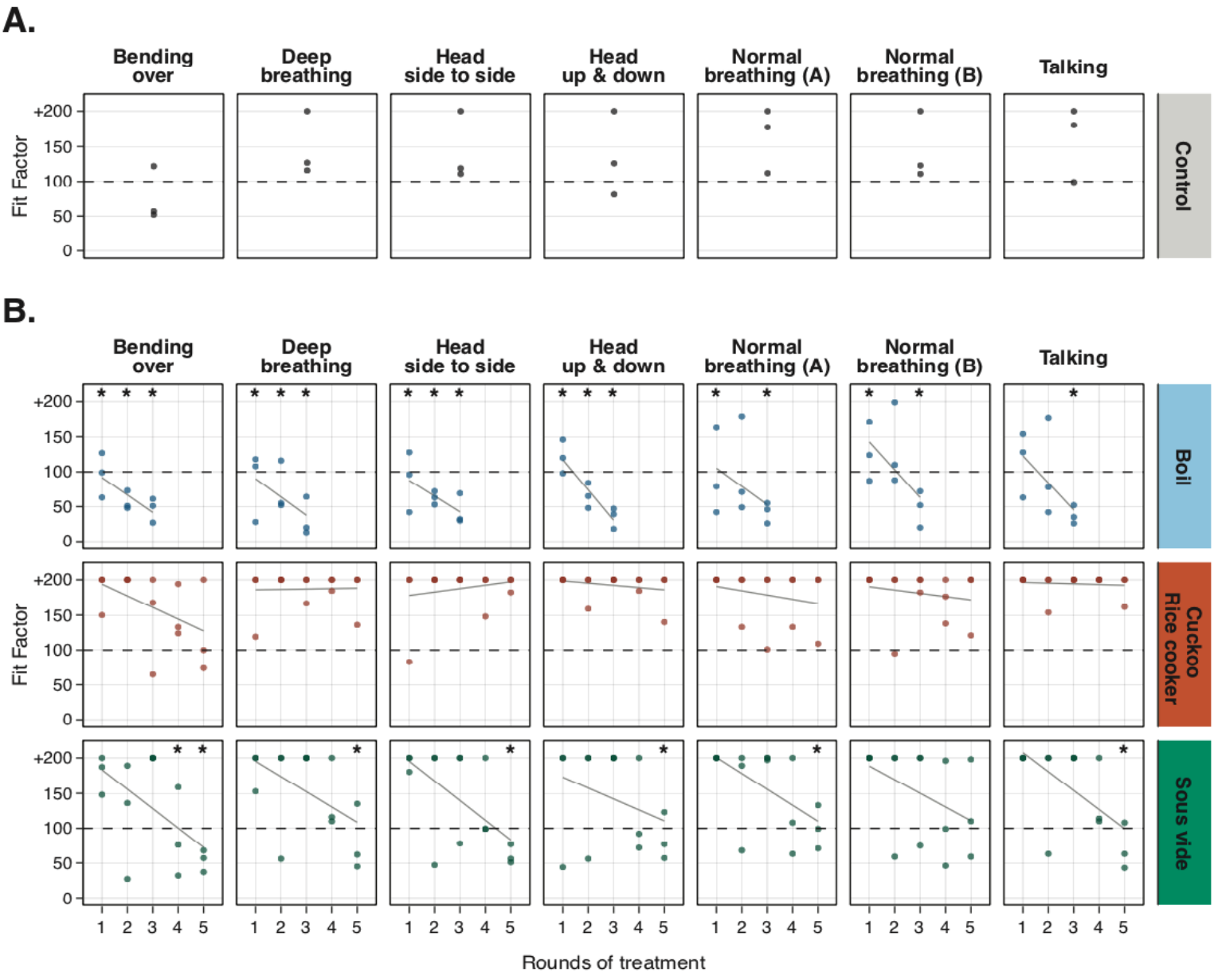

Fig 3. Halyard Fluidshield 3 FFR fit for different testing categories. After exposing FFRs to different methods and repetitions of heat-treatment, the fit for different testing categories was estimated with the PortaCountPro+. The fit was assessed three times for each category (black dots). **(A)** The control FFR was not subjected to any rounds of heat treatment. **(B)** Grey regression line is overlaid for each

treatment method and category (y ~ mx + b) (Table S5 and S6). Analysis of variance p-values shown when there is significant variation in means among treatment category groups and control. Significance (*) $p < 0.05$.

For FFRs decontaminated in the Cuckoo rice cooker, there was a progressive decrease of the fit score ($y = 212–16.8x$, $r2 = 0.24$) when the subject was *bending over* (Fig 3). For FFRs that were boiled ($y = 131–31x$, $r2 = 0.99$) or heated using a sous vide machine ($y = 206–22.8x$, $r2 = 0.66$) there was a progressive decrease in fit score for all categories. For sous vide machine treatment, this trend was strongest when the subject was *bending over* ($y = 212–27.9x$, $r2 =0.34$) or turning their *head side to side* ($y = 224 –28.3x$, $r2 = 0.38$). After three rounds of sous vide machine treatment *bending over* factors were significantly lower than control ($p < 0.05$) but the FFR still passed (i.e., overall fit factor of 100 or greater) the fit test with an overall fit factor of 123. After four rounds of sous vide machine treatment, the FFR failed the fit test with an overall fit factor of 69. The FFR performed significantly worse than the control ($p < 0.05$) in all fit categories but one (*normal breathing*) (Fig 3, Table S4, Table S5, Table S6).

Evaluating the effects of appliance-based heat treatment on FFR filtration performance

To determine whether each of our three heat treatment methods affected the filtration performance of Halyard Fluidshield 3 FFRs, we performed filtration efficiency (FE) analyses on samples of material from each mask that underwent quantitative fit testing. For this analysis, we developed a modified version of the standard NIOSH test (TEB-APR-STP-0059) assessing the penetration of non-neutralized saline aerosols. Particle counts were measured in six different size bins, by a calibrated particle counter (bins of 0.3 μm, 0.5 μm, 1 μm, 2.5 μm, 5 μm, and 10 μm size classes). While this is not the first of such

pipelines [26], our apparatus has all the major design elements needed to normalize for constant flow rates regardless of filter impedance (Fig 4A, Table S7). Furthermore, our experiments were conducted with a steady flow rate per unit area of the filter that exceeds the rates expected under standard NIOSH testing, which generally decreases filtering efficiency compared to lower flow rates [28–30]. Testing was performed on two different central sites on each treated and control mask, with one site directing flow through the fabric to mimic inhalation, and the other site testing flow in the exhalation direction.

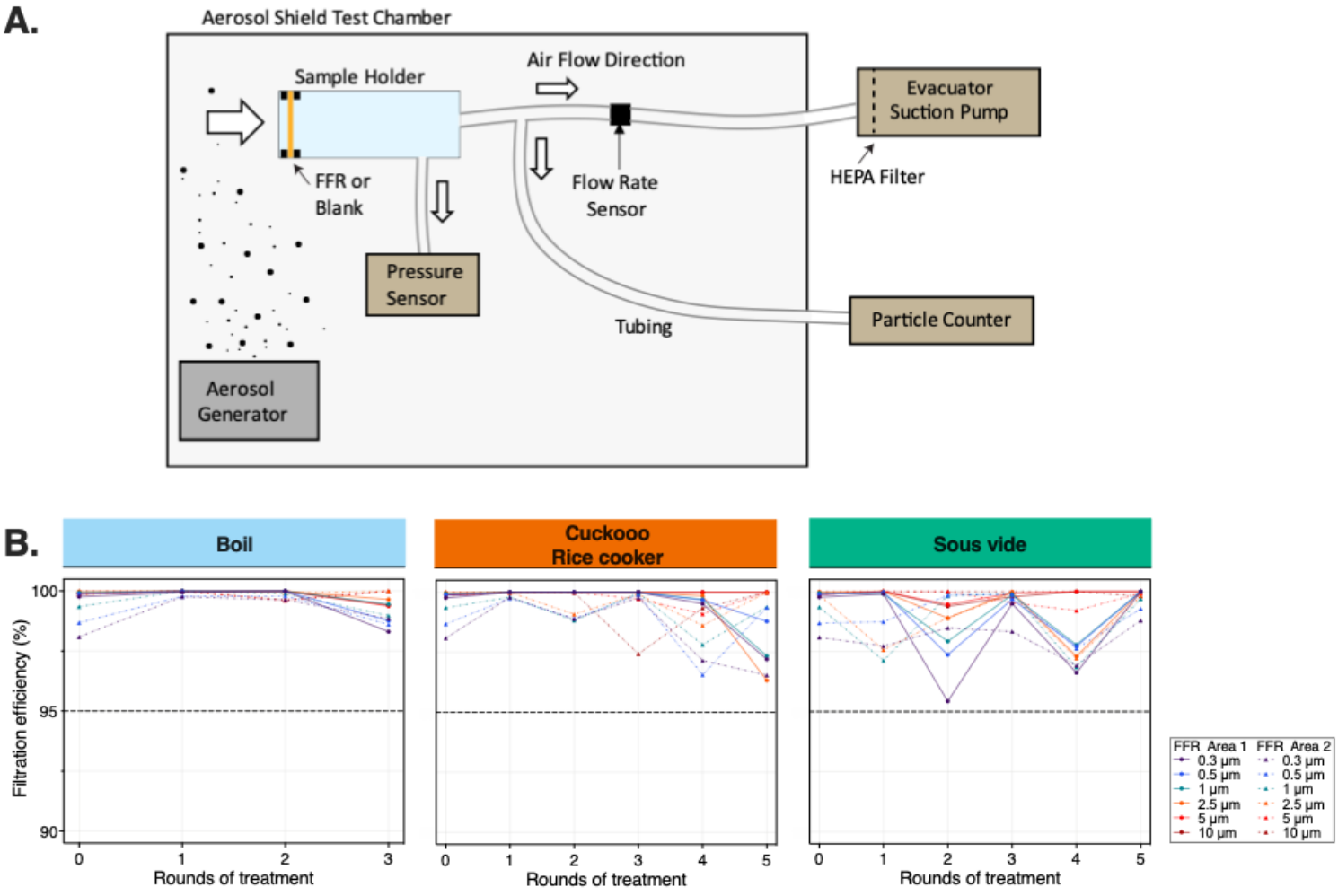

Fig 4. Filtration efficiency for control and heat-treated Halyard Fluidshield 3 FFRs. (**A**) Filtration efficiency test experimental setup. A humidifier confined by an aerosol shield test chamber was used

as an aerosol generator. FFRs were attached to a sample holder and air and any suspended particles were drawn through the FFR by an evacuator suction pump and diverted to a particle counter. FFR impedance was measured through a pressure sensor attached to the sample holder. **(B)** The filtration efficiency for different particle sizes (bins of 0.3 μm, 0.5 μm, 1 μm, 2.5 μm, 5 μm, and 10 μm size classes) were determined for two mask regions of FFRs that were exposed to different methods and repetitions of heat-treatment. None of the treatment methods tested reduces Halyard Fluidshield 3 FFR filtration performance below 95%.

Comparisons between filtration efficiencies in the control and heat-treated FFRs indicate that none of our possible decontamination strategies reduced FFR FE below 95%, meaning that the required performance of 'N-95' FFRs was met by all of our treated masks under our test conditions (Fig 4B, Table S7). We note further that a passing score during any of the quantitative fit testing procedures supports these results, as any damage to the N95 mask material would compromise the overall filterability of the mask and result in the FFR failing the fit test. On the other hand, FE testing also demonstrates that flow and filtration properties of the mask material are not the only important consideration, as proper mask fit is critical to maintain a high level of protection. As both a check of our novel filter test rig and a demonstration of very small leaks significantly affecting effective filter performance, we used an 18-gauge needle to introduce small holes in the filter after normal testing. FE decreased as a function of the number of pinholes introduced into the mask material (Fig S5) and pressure across the N95 FFR material decreased at a flow rate of 10 lpm (Table S8).

DISCUSSION

Pasteurization of pathogens in food and vaccines occurs between 60°C and 70°C for 30 minutes [25] and SARS-CoV-2 has been experimentally inactivated in FFRs after one hour at 70°C [15]. Under these temperature conditions, some FFRs have been shown to preserve fit and filtration efficiency from three to over ten rounds of decontamination using dry heat [15,31]. Here we assessed different heat-based

methods that are likely to deactivate SARS-CoV-2 (Table 1) using common household appliances (Table 2).

We tested two FFR models, the Halyard Fluidshield 3 and the Uniair San Huei, after sequential rounds of heat treatment and performed blinded comparisons of their fit and filtration properties to control, untreated FFRs. The control Uniair San Huei FFR did not fit any of our volunteers and exhibited widely varying fit test results, and was thus excluded from our final analysis of potential decontamination methods. This result emphasizes the importance of regular fit testing, as proper fit is paramount for appropriate protection. For the Halyard Fluidshield 3 FFRs, we measured fit and filtration efficiency after each round of treatment. We found that *bending over* reduces fit factor, and therefore protection, the most (Fig 3). We propose that paying special attention to movement-specific fit testing results when fitting a respirator could aid the end user to adjust their behavior while wearing FFRs (e.g., kneeling vs. bending).

We show that the Halyard Fluidshield 3 fit and filtration efficiency are preserved for up to five rounds of treatment using the *Keep warm* function of a rice cooker with precise temperature control. The CDC does not recommend re-using FFRs more than five times, so we did not subject the respirators to more than five rounds of treatment [10]. Sous vide machine treated masks preserved fit only up to four rounds, possibly because the respirator was slightly deformed by the water and weights. Flow and filtration analysis of treated FFRs demonstrated that none of the heat treatment methods lowered filtration efficiency below the required 95%. Moreover, we found that even the boiled Halyard Fluidshield 3 FFRs tested for this study preserved FE after three rounds of treatment, which is greater than what has

been previously reported [32]. It should be noted that this particular model of FFR, which was designed to protect against fluid splashes in the operating room, is rated as a surgical N95 and is thus considered water-resistant. Further research should be done to determine whether splash-protective respirators are more resistant to changes in FE during humid or water-immersive treatment conditions. Overall, while boiling may be a suitable way to decontaminate FFRs, repeated treatment reduced fit below the passing score much faster than 'dry' heat [9,31].

Our results suggest that at-home appliances are a viable option for decontamination of masks. Since only a limited number of appliances were tested, it is essential for the user to test the selected appliance to guarantee it can reach and maintain 70°C for 60 minutes before attempting decontamination. Such testing can be done in a home environment, for example, by using a precise meat thermometer. As is also the case for commercial decontamination methods, it is essential to carefully examine the FFR after each round of heat exposure to ensure that it has no material damage, burns or tears. As indicated by differences in the goodness of fit between FFR models and between individual FFRs exposed to the same decontamination treatment, it is imperative to carefully examine the FFR before the first use and after each treatment and ensure close fit of the mask all around the face.

It is also important to note that FFRs treated with a dry heat at 70°C decontamination procedure as demonstrated here, will not be sterilized. Pathogens such as *Clostridium difficile* will not be killed and could still pose a risk to public health. Therefore, appliance-heat treated FFRs using methods like the ones described here should always be re-used by the same person [33].

While not recommended for clinical or routine use, the potential decontamination methods evaluated here demonstrate that household appliances could constitute a low-cost strategy for N95 decontamination that could be performed in resource-constrained settings or situations where no viable alternative exists. We note also that our analysis of decontamination conditions and test results on medical-grade FFRs suggest that similar at-home heat-treatment methods would likely be effective for decontaminating other COVID-exposed materials, such as cloth face masks, as long as the same provisions are taken.

MATERIALS AND METHODS

Mask treatment

Testing was performed on two N95 FFR models, the standard Halyard Fluidshield 3 (TC-84A-7521) and the Uniair San Huei SH3500 (TC-84A-4313) (Fig S2). FFRs were randomly assigned to either a treatment group or a control group of untreated masks [15,34]. Potential decontamination protocols were repeated up to five times for masks treated at 70ºC and up to three times for masks that were boiled (Fig 1). The maximum of five rounds of treatment follows the current CDC safety recommendations for FFR reuse as part of crisis capacity and conservation strategies [27]. The Columbia University Institutional Review Board reviewed this study's protocol and determined that ethical approval could be waived (IRB reference AAAT5503).

To heat the FFRs at 70ºC for one hour, we used two different types of home appliances: a rice cooker and a sous vide machine. Temperature within each appliance was recorded for the duration of the treatment using a wireless sensor (Inkbird Thermometer IBS-TH1) for the rice cooker and MeatStick

Wireless Thermometer 4335995327 for the sous vide machine. Both thermometers were benchmarked against a calibrated lab thermometer (Oakton Acorn Series pH 5 Meter and Thermometer) for accuracy. FFRs that were assigned to be decontaminated in the rice cooker were placed in breathable paper bags and the rice cooker was preheated to 70ºC using the *Keep Warm* mode. After the rice cooker reached the specified temperature, the paper bag containing the mask was inserted and the temperature held at 70º C for 60 minutes. For treatment with the sous vide machine, FFRs were sealed in a polypropylene plastic bag (double protection Ziploc© Freezer Bags) before being placed in the water preheated to 70º C. In order to completely submerge the FFR, a 140 g weight was placed on top of the plastic bag. The temperature of the sous vide machine was set to 70ºC for 60 minutes. FFRs subjected to boiling were submerged directly in 1.3 L of boiling water at 100 ºC within a 1.4 L pot and were drained and allowed to air-dry overnight post-treatment (Fig 2, photo panels).

FFR fit test

Quantitative fit tests were performed using the manufacturer provided "N95" setting of a calibrated TSI PortaCount Pro+ Respirator Fit Tester 8038 with ambient particulates and aqueous aerosols produced by an ultrasonic humidifier (NYC tap water). Adherent to the Occupational Safety and Health Administration's (OSHA's) Respiratory Protection Standard (29CFR 1910.134), the Condensation Nuclei Counter (CNC) Quantitative Fit Test for Filtering Facepiece Respirators was used [27]. This test reports a quantitative fit factor score for seven sequential test components (normal breathing, deep breathing, head side to side, head up and down, talking, bending over, and normal breathing) as well as an overall fit factor that is the geometric mean of the seven individual scores. A fit score of ≥ 100 is considered passing in each individual category. Based on the OSHA Respiratory Protection Standard,

an overall fit factor of ≥ 100 is required for passing, regardless of performance (i.e., pass or fail) on each test component [27]. It should be noted that the system gives a maximum possible score of 200+ reported as 201 [34].

The CNC quantitative fit test was performed three times on all FFRs used in the experiment. We obtained a pre-treatment baseline fit factor (blind control) and post-treatment fit tests (also blind) to quantify fit factors and variance. All tests were performed on the same test subject to control for variability in facial features. To minimize user bias, the experimenter and subject were both blinded to which (if any) treatment each mask had undergone. Each mask was punctured and fitted with the commercial metal hose adapter designed for use with the PortaCount Pro+ Respirator Fit Tester 8038 and then coupled via 3/16" vinyl tubing to the Portacount unit. As per CDC recommendations, a user seal check was performed prior to each fit test measurement and adjustments were made until the user deemed that there were no detectable air leaks during forceful breathing [10].

FFR filtration efficiency test

Due to the limited availability of NIOSH test apparatus, a modified version of the standard NIOSH procedure (TEB-APR-STP-0059) was developed to determine the particulate filter efficiency of N95 FFRs (*41*). Respirator filters were challenged by a NaCl aerosol generated using a humidifier (Vicks© Filter-Free Cool Mist Humidifier) filled with 2% saline solution. Non-neutralized particles were released into a polycarbonate test chamber (~150 L volume), which was maintained at a minimum 0.3-μm particle count of 5000 particles per ft^3. Each FFR was manually secured over an iso-KF 25 fitting. After ~10 cm of ~25 mm ID stainless steel tubing, another KF-25 to barbed fitting joined via 3/8" ID

silicone tubing connected to the both the calibrated particle counter (Extech Instruments VCP300) and a high-performance surgical smoke removal device used as an evacuator (Buffalo Filter VisiClear) through a "wye" fitting (Fig 4A). Pressure drop across the filter is monitored with a Sensirion SDP8-500 differential pressure sensor, and the air flow volume is monitored by a Sensirion Mass Flow Meter (part number SFM3300-D). Both devices are read through their I2C communications channel through a custom program running on an Arduino Uno and then recorded on a PC at rates over 10 Hz.

Tests were conducted at a flow rate of 10 lpm with a 4.54 cm^2 area of effective filtration, which exceeds the rate of 85 lpm used during NIOSH testing when our filter patch is scaled proportionally to the area of the entire mask [35]. We compensated for any variation in the impedance of the mask material by changing the strength of the suction of the evacuator to obtain a flow rate of 10 lpm through each mask or blank (nozzle open to allow for unimpeded ambient air flow) prior to each filtration test.

Before measuring the filtration efficiency of each decontaminated or control FFR, the baseline ambient particle count within the aerosol shield chamber was measured as the particle count downstream of an open nozzle. First, particles were suctioned through either a blank or mask at a flow rate of 10 lpm for 20 seconds, then the suction was switched off. Then, following a 5 second pre-counting sample draw, the cumulative number of same-sized particles downstream of each mask or blank were counted over a 20 second sampling period at a 2.83 lpm sampling rate controlled by the particle counter's internal pump. The total volume of the internal tubing, sensors, and stainless port was ~1.35 liters, and designed such that the bulk of the air sampled by the particle counter during its total 25 second counter operation was air drawn through the filter unit at the 10 lpm volume flow rate, not air drawn through the filter

by the pump action of the particle counter. Particles binned into 0.3 μm, 0.5 μm, 1 μm, 2.5 μm, 5 μm, and 10 μm size classes were measured. The filtration efficiency (FE) was calculated using the equation,

$$Filtration\ Efficiency\ (FE)\ =\ (1\ -\ \frac{C_{mask}}{C_{chamber}})\ \times\ 100\%$$

where C_{mask} and $C_{chamber}$ denote the concentrations of particles of the same size downstream of the mask and within the aerosol chamber, respectively. For each FFR, flow test measurements of two different central N95 material areas were obtained to sample the variance.

To assess the sensitivity of our modified flow test, the filtration efficiency of an untreated control FFR before and after introducing damage was measured using the same experimental setup and methodology as described above. Filtration efficiency test sensitivity was determined in two mask areas that were punctured with an 18-gauge needle one to three times (Fig S5, Table S8). Each puncture was at most 0.3% of the filter area, yet reduced filtering efficiency of the 0.3 um particles by roughly 25% (e.g., from >95% to 75%). This large reduction in efficiency from such a small leak highlights the importance of proper fit, with no voids, for effective protection.

Statistical analysis

All statistical analyses were run in the R software environment (v4.0.1). The decrease of fit factors over repeated treatment was evaluated using linear regressions (stat_smooth function, method=lm, ggplot2 v3.3.0). Variance component analyses were calculated with nested one-Way ANOVA (aov(score~treatment+Error(mask)). F-values and significance levels for the F-statistics reported [36].

REFERENCES:

1. Cook, T. M. Personal protective equipment during the coronavirus disease (COVID) 2019 pandemic – a narrative review. *Anaesthesia* **75**, 920–927 (2020).

2. Santarpia, J. L. *et al.* The Infectious Nature of Patient-Generated SARS-CoV-2 Aerosol.

3. Tabah, A. *et al.* Personal protective equipment and intensive care unit healthcare worker safety in the COVID-19 era (PPE-SAFE): An international survey. *J Crit Care* **59**, 70–75 (2020).

4. CDC. Infection Control Guidance for Healthcare Professionals about Coronavirus (COVID-19). https://www.cdc.gov/coronavirus/2019-ncov/hcp/infection-control.html (2020).

5. Wang, X., Pan, Z. & Cheng, Z. Association between 2019-nCoV transmission and N95 respirator use. *J Hosp Infect* **105**, 104–105 (2020).

6. Srivastava, N. & Saxena, S. K. Prevention and Control Strategies for SARS-CoV-2 Infection. *Coronavirus Disease 2019 (COVID-19): Epidemiology, Pathogenesis, Diagnosis, and Therapeutics* 127–140 (2020) doi:10.1007/978-981-15-4814-7_11.

7. CDC. Recommended Guidance for Extended Use and Limited Reuse of N95 Filtering Facepiece Respirators in Healthcare Settings. https://www.cdc.gov/niosh/topics/hcwcontrols/RecommendedGuidanceExtUse.html (2020).

8. FDA. Enforcement Policy for Face Masks and Respirators During the Coronavirus Disease (COVID-19) Public Health Emergency (Revised). https://www.fda.gov/media/136449/download (2020).

9. Juang, P. S. C. & Tsai, P. N95 Respirator Cleaning and Reuse Methods Proposed by the Inventor of the N95 Mask Material. *J Emerg Medicine* **58**, 817–820 (2020).

10. CDC. COVID-19 Decontamination and Reuse of Filtering Facepiece Respirators. https://www.cdc.gov/coronavirus/2019-ncov/hcp/ppe-strategy/archived-decontamination-reuse-respirators.html (2020).

11. Andersen, B. M., Bånrud, H., Bøe, E., Bjordal, O. & Drangsholt, F. Comparison of UV C Light and Chemicals for Disinfection of Surfaces in Hospital Isolation Units. *Infect Control Hosp Epidemiology* **27**, 729–734 (2006).

12. N95Decon. Heat and Humidity for Bioburden Reduction of N95 Filtering Facepiece Respirators. www.n95decon.org/files/heat-humidity-technical report.

13. Daeschler, S. C. *et al.* Effect of moist heat reprocessing of N95 respirators on SARS-CoV-2 inactivation and respirator function. *Cmaj* **192**, E1189–E1197 (2020).

14. Kumar, A. *et al.* N95 Mask Decontamination using Standard Hospital Sterilization Technologies. doi:10.1101/2020.04.05.20049346.

15. Fischer, R. *et al.* Assessment of N95 respirator decontamination and re-use for SARS-CoV-2. (2020).

16. Rockey, N. *et al.* Humidity and Deposition Solution Play a Critical Role in Virus Inactivation by Heat Treatment of N95 Respirators. *Msphere* **5**, (2020).

17. Massey, T. *et al.* Quantitative form and fit of N95 filtering facepiece respirators are retained and coronavirus surrogate is inactivated after heat treatments. doi:10.1101/2020.04.15.20065755.

18. Lore, M. B., Heimbuch, B. K., Brown, T. L., Wander, J. D. & Hinrichs, S. H. Effectiveness of Three Decontamination Treatments against Influenza Virus Applied to Filtering Facepiece Respirators. *Ann Occup Hyg* **56**, 92–101 (2012).

19. Anderegg, L. *et al.* A scalable method of applying heat and humidity for decontamination of N95 respirators during the COVID-19 crisis. *Plos One* **15**, e0234851 (2020).

20. Straten, B. van *et al.* Sterilization of disposable face masks by means of standardized dry and steam sterilization processes; an alternative in the fight against mask shortages due to COVID-19. *J Hosp Infect* **105**, 356–357 (2020).

21. appliances, G. E. Wall ovens and ranges. https://products.geappliances.com/appliance/gea-support-search-content?contentId=18501.

22. Gluesenkamp, K. *Residential Clothes Dryer Performance Under Timed and Automatic Cycle Termination Test Procedures*. https://web.ornl.gov/sci/buildings/docs/2014-10-09-ORNL-DryerFinalReport-TM-2014-431.pdf (2014).

23. Pascoe, M. J. *et al.* Dry heat and microwave generated steam protocols for the rapid decontamination of respiratory personal protective equipment in response to COVID-19-related shortages. *J Hosp Infect* **106**, 10–19 (2020).

24. Viscusi, D. J., Bergman, M. S., Eimer, B. C. & Shaffer, R. E. Evaluation of Five Decontamination Methods for Filtering Facepiece Respirators. *Ann Occup Hyg* **53**, 815–827 (2009).

25. Vieira, F. R. & Pecchia, J. A. An Exploration into the Bacterial Community under Different Pasteurization Conditions during Substrate Preparation (Composting–Phase II) for Agaricus bisporus Cultivation. *Microbial Ecol* **75**, 318–330 (2018).

26. Konda, A. *et al.* Aerosol Filtration Efficiency of Common Fabrics Used in Respiratory Cloth Masks. *Acs Nano* **14**, 6339–6347 (2020).

27. OSHA. 1910.134 - Respiratory Protection. https://www.osha.gov/laws-regs/regulations/standardnumber/1910/1910.134 (2011).

28. Gao, S. *et al.* Penetration of Combustion Aerosol Particles Through Filters of NIOSH-Certified Filtering Facepiece Respirators (FFRs). *J Occup Environ Hyg* **12**, 678–685 (2015).

29. Eninger, R. M. *et al.* Filter Performance of N99 and N95 Facepiece Respirators Against Viruses and Ultrafine Particles. *Ann Occup Hyg* **52**, 385–396 (2008).

30. Huang, S.-H. *et al.* Factors Affecting Filter Penetration and Quality Factor of Particulate Respirators. *Aerosol Air Qual Res* **13**, 162–171 (2013).

31. Liao, L. *et al.* Can N95 Respirators Be Reused after Disinfection? How Many Times? *Acs Nano* **14**, 6348–6356 (2020).

32. Ou, Q., Pei, C., Kim, S. C., Abell, E. & Pui, D. Y. H. Evaluation of decontamination methods for commercial and alternative respirator and mask materials – view from filtration aspect. *J Aerosol Sci* **150**, 105609 (2020).

33. Kazanowski, M., Smolarek, S., Kinnarney, F. & Grzebieniak, Z. Clostridium difficile: epidemiology, diagnostic and therapeutic possibilities—a systematic review. *Tech Coloproctol* **18**, 223–232 (2014).

34. CDC. Determination of Particulate Filter Penetration Test Powered Air-Purifying Respirator Filters Standard Testing Procedure (STP). https://www.cdc.gov/niosh/npptl/stps/pdfs/TEB-APR-STP-0001-508.pdf.

35. Brosseau, L. M., McCullough, N. V. & Vesley, D. Mycobacterial Aerosol Collection Efficiency of Respirator and Surgical Mask Filters under Varying Conditions of Flow and Humidity. *Appl Occup Environ Hyg* **12**, 435–445 (1997).

36. Crawley, M. J. *Statistics: An Introduction Using R*. (Wiley).

LEGENDS:

MAIN FIGURE LEGENDS:

Fig 1. Experimental workflow for Halyard Fluidshield 3 (TC-84A-7521) FFRs. (A) Each FFR was blind assigned to either **(B)** *x* round(s) of appliance-based heat treatment OR to a control group. We tested three appliance-based heat treatment methods: Cuckoo rice cooker, sous vide machine and boiling. Boiled FFRs were treated up to three times. FFRs heated with sous vide machine and Cuckoo rice cooker were treated up to five times. Control FFRs were not exposed to any treatment. **(C)** Treatment-exposed and control FFRs were fit tested using the built-in N95 setting of a TSI PortaCount Pro+ Respirator Fit Tester 8038. Three technical replicate measurements were taken for each FFR and overall Fit Factors (Fig 2) and fit values for the different testing categories (Fig 3) were recorded. **(D)** The effect of appliance-based heat treatment on FFR filtration performance was evaluated for treatment and control FFRs using a modified version of the standard NIOSH test (Fig 4). Filtration efficiency was tested on two different FFR areas. For the Uniair San Huei SH3500 (TC-84A-4313) model, FFRs were only exposed to heat using the Cuckoo rice cooker and the sous vide machine. They were treated up to three times. Fit was estimated for both treatment and control FFRs as it is described in **(C)**, the masks were not tested for filtration performance.

Fig 2. Average Halyard Fluidshield 3 FFR fit factor. After exposing FFRs to different methods and repetitions of heat-treatment, the fit factor was estimated with the PortaCountPro+. The fit factor was estimated three times for each FFR (smaller dots) and average fit factor is reported to the nearest integer (red bar). The control FFR was not subjected to any rounds of heat treatment. Grey regression line is overlaid for each treatment method ($y \sim mx + b$). Analysis of variance p-values is shown when there is significant variation in means among treatment group and control. Significance (*) $p < 0.05$. Photographs of the heat generation appliances shown in the panel below their respective fit factor profile.

Fig 3. Halyard Fluidshield 3 FFR fit for different testing categories. After exposing FFRs to different methods and repetitions of heat-treatment, the fit for different testing categories was estimated with the PortaCountPro+. The fit was assessed three times for each category (black dots). **(A)** The control FFR was not subjected to any rounds of heat treatment. **(B)** Grey regression line is overlaid for each treatment method and category ($y \sim mx + b$) (Table S5 and S6). Analysis of variance p-values shown when there is significant variation in means among treatment category groups and control. Significance (*) $p < 0.05$.

Fig 4. Filtration efficiency for control and heat-treated Halyard Fluidshield 3 FFRs. (A) Filtration efficiency test experimental setup. A humidifier confined by an aerosol shield test chamber was used as an aerosol generator. FFRs were attached to a sample holder and air and any suspended particles were drawn through the FFR by an evacuator suction pump and diverted to a particle counter. FFR impedance was measured through a pressure sensor attached to the sample holder. **(B)** The filtration efficiency for different particle sizes (bins of 0.3 μm, 0.5 μm, 1 μm, 2.5 μm, 5 μm, and 10 μm size classes) were determined for two mask regions of FFRs that were exposed to different methods and repetitions

of heat-treatment. None of the treatment methods tested reduces Halyard Fluidshield 3 FFR filtration performance below 95%.

MAIN TABLE LEGENDS:

MAIN TABLE LEGENDS:

Table 1. Effect of heat and humidity on enveloped viruses on N95 FFRs. Log viral reduction >3 is sufficient to consider the virus inactivated. N/A: Not Applicable, the parameter was not tested. DMEM refers to Dulbecco's Modified Eagle Medium.

Table 2. Temperature maintained after initial heating period in the appliances tested. The Cuckoo (CR-0655F) *Keep Warm* setting maintained an average temperature of 71.7°C (-2.0°C /+0.5°C). The sous vide AuAg Immersion Circulator (A808, 950 W) has an average temperature of 69.8°C (-1.6°C /+0.4°C). The Aroma (ARC-743-1NGB) *Keep Warm* setting reached an average temperature of 67.5°C (-4.0°C /+2.0°C).

ACKNOWLEDGMENTS:

We thank Richard Hormigo for circuit design for the filtration efficiency testing rig; David Brenner for helpful discussions; VisiClear for the Buffalo Filter VisiClear; Zuckerman Institute and Columbia Environmental Health and Safety for the space to perform experiments; Columbia Researchers Against COVID-19 for assembling this team; Wearing is Caring; Peter Andolfatto, Rui Costa, Ivaylo Ivanov, and Andrés Bendesky for support throughout the project; Anil Lalwani for providing the FFRs used in this study.

FUNDING:

The Zuckerman Mind Brain Behavior Institute, Columbia University provided funding to support this project.

AUTHOR CONTRIBUTIONS:

T.X.C, A.P, D.S.P and E.M.C.H conceived the study and designed the experiments. T.X.C. and A.P. performed the experiments, analyzed the data and wrote the manuscript. K.Y-M. performed the literature survey. T.X.C, A.P, E.M.C.H and L.E. made the figures. D.S.P. designed and assembled the FFR filtration efficiency test and provided training. N.A.S, J.H. and L.W. provided specialist support. S.F. provided training on the PortaCountPro+. All the authors commented and edited the manuscript.

COMPETING INTERESTS:

The authors declare no competing interests.

DATA AVAILABILITY:

All data is available in the main text or the supplementary materials.

LIST OF SUPPLEMENTARY MATERIALS:

- Supplementary Figs S1 – S5
- Supplementary Tables S1 – S8

SUPPLEMENTARY FIGURES:

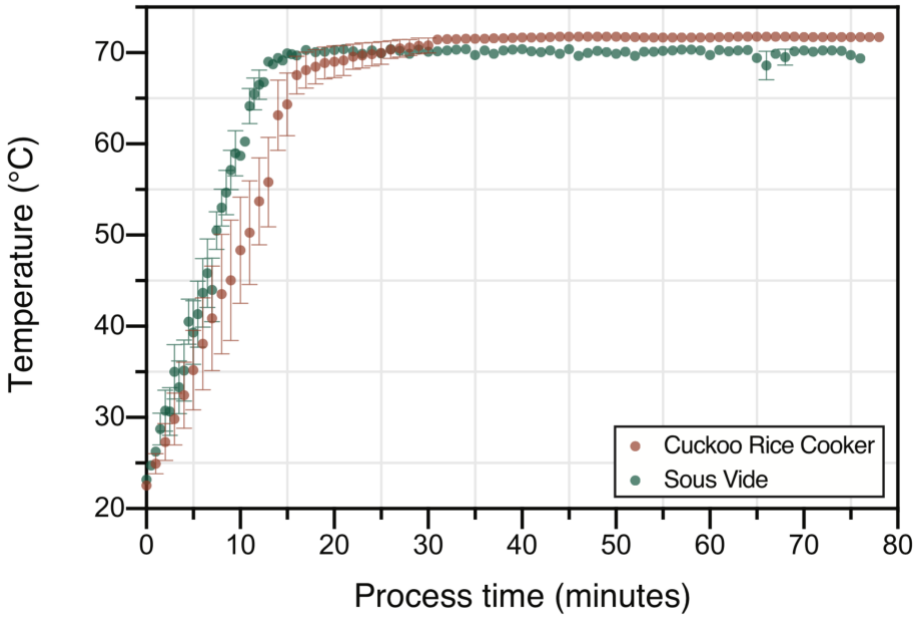

Fig S1. Average temperature profile of FFRs over one round of treatment. Temperature was recorded for the duration of the treatment using a wireless sensor (Inkbird Thermometer IBS-TH1 for the rice cooker and MeatStick Wireless Thermometer 4335995327 for the sous vide machine).

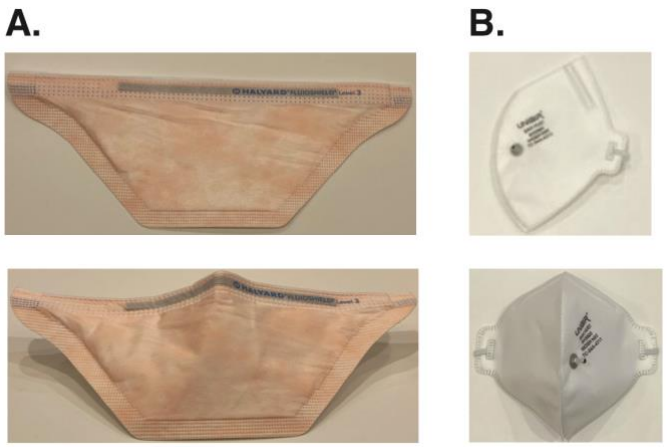

Fig S2. FFR models. (A) Halyard Fluidshield 3 FFR. **(B)** Uniair San Huei FFR. Port for quantitative fit testing visible in the photo.

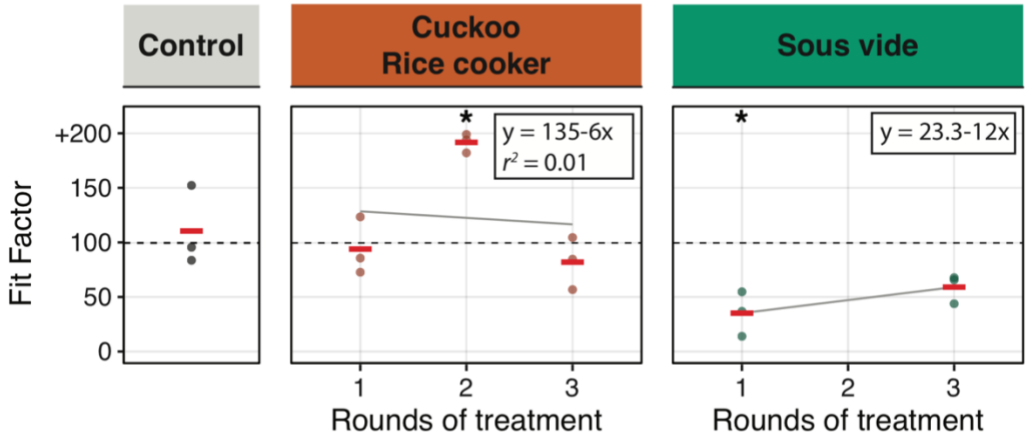

Fig S3. Average FFR fit factor Uniair San Huei. After exposing FFRs to several methods and rounds of treatment, the fit factor was estimated with the PortaCountPro+. The fit factor was estimated three times for each FFR (smaller dots) and the average fit factor is reported to the nearest integer (red bar). The control FFR was not subjected to any round of treatment. Grey regression line is overlaid for each treatment method (y ~ mx + b) (Table S2). Analysis of variance p-values is shown when there is significant variation in means among treatment group and control. Significance (*) $p < 0.05$.

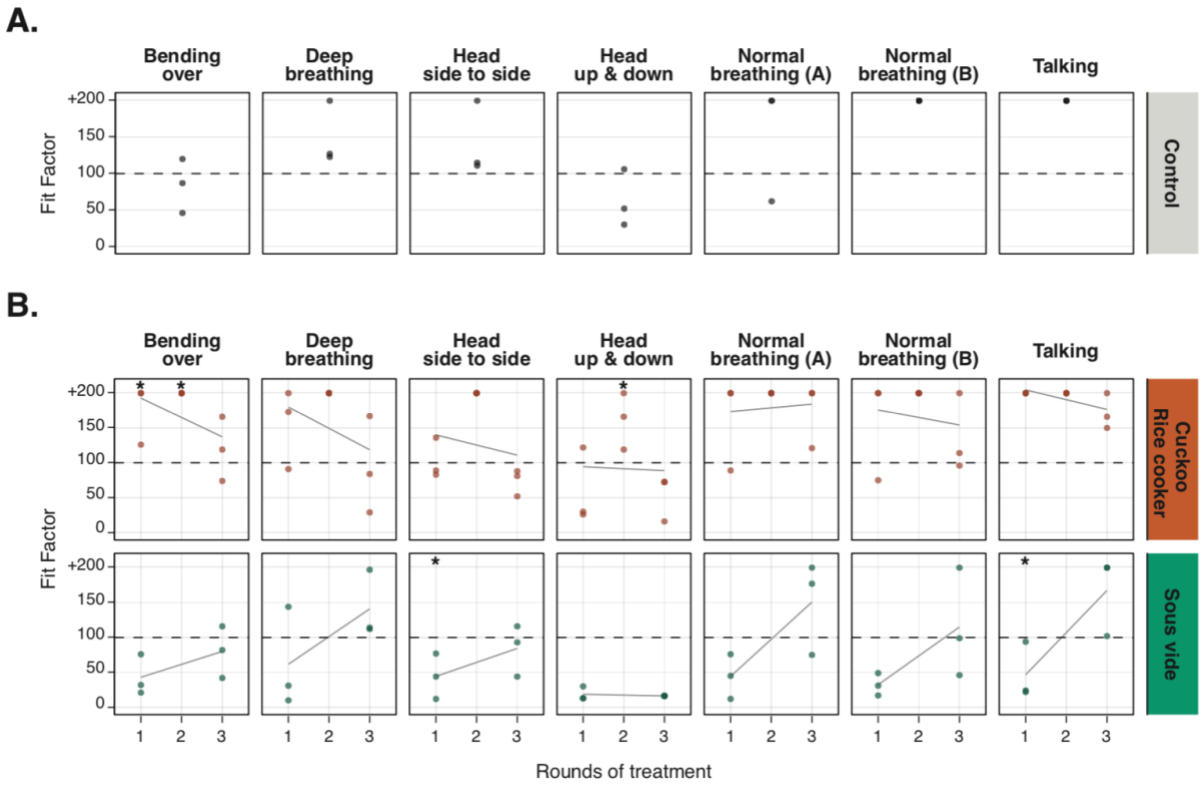

Fig S4. Uniair San Huei FFR fit for different testing categories. After exposing FFRs to several methods and rounds of treatment, the fit for different testing categories was estimated with the PortaCountPro+. The fit was estimated three times for each category (black dots). **(A)** The control FFR was not subjected to any round of treatment. Grey regression line is overlaid for each treatment method and category ($y \sim mx + b$) (Table S3). **(B)** Analysis of variance p-values shown when there is significant variation in means among treatment groups and control. Significance (*) $p < 0.05$.

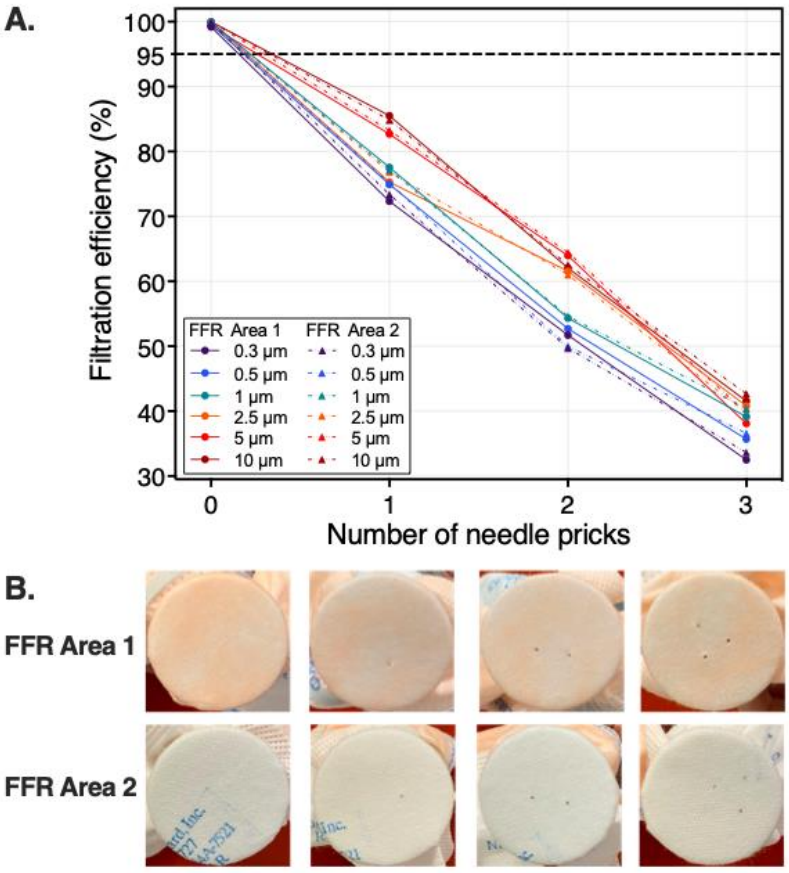

Fig S5. Filtration efficiency for control and punctured Halyard Fluidshield 3 FFRs. (A) The filtration efficiency of two N95 mask areas for different particle sizes (bins of 0.3 µm, 0.5 µm, 1 µm, 2.5 µm, 5 µm, and 10 µm size classes) were determined for an untreated FFR before and after puncturing with an 18-gauge needle once, twice, and three times. **(B)** The front view of two FFR mask regions subject to punctures, fitted to the sample holder, and tested for filtration efficiency is shown.

SUPPLEMENTARY TABLES S1 – S8

Rounds of treatment	Treatment	Fit Factor			Average Fit Factor	p-value	F statistic	Regression line and r^2
		Technical replicate 1	Technical replicate 2	Technical replicate 3				
0	Control	108	184	94	129	-	-	-
1	Boil	51	141	105	99	0.02	12.54	$y = 131–31x$, $r^2 = 0.99$
2		54	86	73	71	0.00	123.67	
3		33	55	23	37	0.00	196.67	
1	Cuckoo Rice cooker	+200	167	175	181	0.31	1.32	$y = 187–4.1x$, $r^2 = 0.67$
2		167	192	187	182	0.28	1.53	
3		165	+200	154	173	0.24	1.93	
4		184	173	176	178	0.08	5.70	
5		144	143	+200	162	0.18	2.57	
1	Sous vide	129	+200	188	172	0.39	0.91	$y = 206–22.8x$, $r^2 = 0.66$
2		49	186	199	145	0.37	1.04	
3		+200	+200	137	179	0.53	0.47	
4		78	98	193	123	0.12	3.89	
5		72	76	59	69	0.00	36.76	

Table S1. Average Halyard Fluidshield 3 FFR fit factor and technical replicates. After exposing FFRs to several methods and rounds of treatment, the fit factor was estimated with the PortaCountPro+. The fit factor was estimated three times for each FFRs and the average fit factor is reported to the nearest integer. Control FFR was not subjected to any round of treatment. Analysis of variance p-values shown for variation in means among treatment group and control. Values rounded to two decimal places. Grey regression line overlaid for each treatment method and category ($y \sim mx + b$) in Fig 2.

Rounds of treatment	Treatment	Fit Factor			Average Fit Factor	p-value	F statistic	Regression line and r^2 (x=reps)
		Technical replicate 1	Technical replicate 2	Technical replicate 3				
0	Control	96	84	153	111	-	-	-
1	Cuckoo Rice cooker	73	86	124	94.3	0.56	0.4	$y = 135–6x$, $r^2 = 0.01$
2		183	+200	195	192.6	0.02	13.94	
3		85	105	57	82.3	0.32	1.27	
1	Sous vide	55	37	14	35.3	0.04	9.64	$y = 23.3–12x$, $r^2 = 1$
2		-	-	-	-	-	-	
3		73	86	124	59.3	0.08	5.21	

Table S2. Average FFR fit factor and technical replicates Uniair San Huei

After exposing FFRs to several methods and rounds of treatment, the fit factor was estimated with the PortaCountPro+. The fit factor was estimated three times for each FFRs and the average fit factor is reported to the nearest integer. The control FFR was not subjected to any round of treatment. Analysis of variance p-values shown for variation in means among treatment group and control. Values rounded to two decimal places. Grey regression line overlaid for each treatment method and category (y ~ mx + b) in Fig S3.

Treatment	Category	Rounds of treatment	p-value	F statistics	Regression line and r^2, (x=reps)
Cuckoo Rice cooker	Bending over	1	0.05	7.76	$y = 221–28.8x$, $r^2 = 0.26$
		2	0.01	29.20	
		3	0.36	1.07	
	Deep breathing	1	0.92	0.01	$y = 211\text{-}30.7x$, $r^2 = 0.17$
		2	0.12	3.99	
		3	0.30	1.44	
	Head side to side	1	0.31	1.38	$y = 154\text{-}14.5x$, $r^2 = 0.04$
		2	0.12	3.99	
		3	0.09	4.84	
	Head up & down	1	0.94	0.01	$y = 97.2\text{-}2.83x$, $r^2 = 0.001$
		2	0.04	9.23	
		3	0.77	0.09	
	Normal breathing (A)	1	0.89	0.02	$y = 168+5.33x$, $r^2 = 0.01$
		2	0.37	1.00	
		3	0.73	0.14	
	Normal breathing (B)	1	0.37	1.00	$y = 187–10.8x$, $r^2 = 0.03$
		2	0.37	1.00	
		3	0.12	3.89	
	Talking	1	0.37	1.00	$y = 219–14x$, $r^2 = 0.41$
		2	0.37	1.00	
		3	0.13	3.61	
Sous vide	Bending over	1	0.20	2.31	$y = 24.5+18.5x$, $r^2 = 0.32$
		3	0.89	0.02	
	Deep breathing	1	0.14	3.31	$y = 22+39.7x$, $r^2 = 0.39$
		3	0.82	0.06	
	Head side to side	1	0.05	7.98	$y = 24.3–20x$, $r^2 = 0.33$
		3	0.18	2.57	
	Head up & down	1	0.13	3.57	$y = 19.8–1.17x$, $r^2 = 0.04$
		3	0.11	4.21	
	Normal breathing (A)	1	0.09	4.89	$y = \text{-}8.83+53.2x$, $r^2 = 0.61$
		3	0.96	0.00	
	Normal breathing (B)	1	0.00	327.65	$y = \text{-}9+41.3x$, $r^2 = 0.45$
		3	0.13	3.54	
	Talking	1	0.00	41.95	$y = \text{-}13.7+60.3x$, $r^2 = 0.69$
		3	0.37	1.00	

Table S3. Analysis of variance among treatment category groups and control Uniair San Huei. Analysis of variance p-values variation in means among treatment category groups and control. Grey regression line overlaid for each treatment method and category (y ~ mx + b) in Fig S4.

Rounds of treatment	Treatment	Technical replicate	Bending over	Deep breathing	Head side to side	Head up & down	Normal breathing (A)	Normal breathing (B)	Talking
0	Control	1	52	116	111	126	178	123	181
		2	122	+200	+200	+200	+200	+200	+200
		3	57	127	119	81	112	111	99
1	Boil	1	63	28	42	98	42	87	63
		2	127	118	128	146	163	172	154
		3	99	108	96	120	79	124	128
2		1	51	52	53	48	71	88	42
		2	73	116	63	65	180	110	78
		3	48	55	72	84	49	+200	178
3		1	61	20	32	39	26	72	26
		2	51	64	69	47	55	52	52
		3	27	13	30	18	46	20	35
1	Cuckoo Rice cooker	1	+200	+200	+200	+200	+200	+200	+200
		2	+200	+200	83	+200	+200	+200	+200
		3	150	119	+200	+200	+200	+200	+200
2		1	+200	+200	+200	+200	133	+200	+200
		2	+200	+200	+200	+200	+200	+200	154
		3	+200	+200	+200	159	+200	95	+200
3		1	168	167	+200	+200	101	183	+200
		2	+200	+200	+200	+200	+200	+200	+200
		3	65	+200	+200	+200	+200	+200	+200
4		1	133	+200	+200	+200	+200	177	+200
		2	124	185	148	185	+200	+200	+200
		3	195	+200	+200	+200	133	138	+200
5		1	74	+200	183	+200	+200	121	162
		2	100	136	+200	140	109	+200	+200
		3	+200	+200	+200	+200	+200	+200	+200
1	Sous vide	1	188	153	+200	44	+200	+200	+200
		2	+200	+200	+200	+200	+200	+200	+200
		3	148	+200	181	+200	+200	+200	+200
2		1	27	56	47	56	68	59	63
		2	136	+200	+200	+200	190	+200	+200
		3	190	+200	+200	+200	+200	+200	+200
3		1	+200	+200	+200	+200	198	+200	+200
		2	+200	+200	+200	+200	+200	+200	+200

		3	+200	+200	78	+200	+200	75	+200
		1	32	110	99	72	63	46	114
4		2	76	116	99	92	108	99	110
		3	159	+200	+200	+200	+200	197	+200
		1	68	45	77	123	99	199	43
5		2	37	135	56	77	133	110	108
		3	57	62	51	57	71	59	63

Table S4. Halyard Fluidshield 3 FFR fit for different testing categories. After exposing FFRs to several methods and rounds of treatment, the fit for different testing categories was estimated with the PortaCountPro+. The fit was estimated three times for each category. Control FFRs was not subjected to any round of treatment.

Treatment	Bending over	Deep breathing	Head side to side	Head up & down	Normal breathing (A)	Normal breathing (B)	Talking
Boil	$y = 117–25x$ $r^2 = 0.52$	$y = 110–26.2x$ $r^2 = 0.30$	$y = 110–22.5x$ $r^2 = 0.38$	$y = 161–43.3x$ $r^2 = 0.82$	$y = 131–26.2x$ $r^2 = 0.17$	$y = 182–39.8x$ $r^2 = 0.37$	$y = 161–38.7x$ $r^2 = 0.36$
Cuckoo Rice cooker	$y = 212–16.8x$ $r^2 = 0.24$	$y = 186+0.6x$ $r^2 = 0.001$	$y = 174+4.9x$ $r^2 = 0.05$	$y = 203–3.2x$ $r^2 = 0.06$	$y = 198–6.13x$ $r^2 = 0.06$	$y = 196–4.7x$ $r^2 = 0.04$	$y = 198–1.03x$ $r^2 = 0.01$
Sous vide	$y = 212–27.9x$ $r^2 = 0.34$	$y = 218–21.9x$ $r^2 = 0.28$	$y = 224–28.3x$ $r^2 = 0.38$	$y = 189–15.7x$ $r^2 = 0.02$	$y = 224–22.9x$ $r^2 = 0.34$	$y = 209–19.6x$ $r^2 = 0.19$	$y = 236–27.3x$ $r^2 = 0.41$

Table S5. Regression line and r^2: Halyard Fluidshield 3 FFR fit for different testing categories. Grey regression line overlaid for each treatment method and category (y ~ mx + b) in Fig 2.

Treatment	Category	Rounds of treatment	p-value	F statistics
Boil	Bending over	1	0.00	31.93
		2	0.00	332.30
		3	0.00	234.99
	Deep breathing	1	0.02	16.68
		2	0.00	36.90
		3	0.00	111.65
	Head side to side	1	0.01	20.04
		2	0.00	635.47
		3	0.00	153.94
	Head up & down	1	0.00	32.98
		2	0.00	169.38
		3	0.00	369.88
	Normal breathing (A)	1	0.04	8.82
		2	0.07	6.22
		3	0.00	342.68
	Normal breathing (B)	1	0.04	8.88
		2	0.12	3.98
		3	0.00	102.08
	Talking	1	0.22	2.17
		2	0.21	2.19
		3	0.01	21.18
Cuckoo Rice cooker	Bending over	1	0.37	1.00
		2	0.37	1.00
		3	0.24	1.89
		4	0.09	5.09
		5	0.12	3.85
	Deep breathing	1	0.37	1.00
		2	0.37	1.00
		3	0.37	1.00
		4	0.37	1.00
		5	0.37	1.00
	Head side to side	1	0.37	1.00
		2	0.37	1.00
		3	0.37	1.00
		4	0.37	1.00
		5	0.37	1.00
	Head up & down	1	0.37	1.00
		2	0.37	1.00
		3	0.37	1.00
		4	0.37	1.00
		5	0.37	1.00
	Normal breathing (A)	1	0.37	1.00

		2	0.37	1.00
		3	0.37	1.00
		4	0.37	1.00
		5	0.37	1.00
	Normal breathing (B)	1	0.37	1.00
		2	0.37	1.00
		3	0.37	1.00
		4	0.19	2.50
		5	0.37	1.00
	Talking	1	0.37	1.00
		2	0.72	0.15
		3	0.37	1.00
		4	0.37	1.00
		5	0.65	0.24
Sous vide	Bending over	1	0.24	1.90
		2	0.16	3.02
		3	0.37	1.00
		4	0.04	9.05
		5	0.00	262.46
	Deep breathing	1	0.37	1.00
		2	0.37	1.00
		3	0.37	1.00
		4	0.12	3.99
		5	0.01	19.00
	Head side to side	1	0.37	1.00
		2	0.37	1.00
		3	0.37	1.00
		4	0.12	4.00
		5	0.00	307.45
	Head up & down	1	0.37	1.00
		2	0.37	1.00
		3	0.37	1.00
		4	0.12	3.92
		5	0.00	34.84
	Normal breathing (A)	1	0.37	1.00
		2	0.32	1.00
		3	0.37	1.00
		4	0.13	3.59
		5	0.01	31.12
	Normal breathing (B)	1	0.37	1.00
		2	0.37	1.00
		3	0.37	1.00
		4	0.12	3.87
		5	0.13	3.67
	Talking	1	0.37	1.00
		2	0.76	0.11
		3	0.37	1.00

	4	0.49	0.57
	5	0.04	8.76

Table S6. Analysis of variance among treatment category groups and control Halyard Fluidshield 3 FFRs. Analysis of variance p-values variation in means among treatment groups and control.

Treatment	Rounds of treatment	Filtration Efficiency (FE)			Pressure Drop	
		Particle Size (μm)	F.E. of FFR Area 1 (%)	F.E. of FFR Area 2 (%)	FFR Area 1 (mmH2O)	FFR Area 1 (mmH2O)
Control	0	0.3	99.76	98.09	38.1	38.1
		0.5	99.88	98.68		
		1	99.94	99.35		
		2.5	99.98	99.85		
		5	99.89	99.89		
		10	99.88	100.00		
Boil	1	0.3	99.95	99.77	33.0	30.5
		0.5	100.00	99.78		
		1	100.00	100.00		
		2.5	100.00	100.00		
		5	100.00	100.00		
		10	100.00	100.00		
	2	0.3	100.00	99.64	38.1	30.5
		0.5	100.00	99.80		
		1	100.00	99.89		
		2.5	100.00	99.92		
		5	100.00	99.61		
		10	100.00	99.64		
	3	0.3	98.31	98.85	35.6	27.9
		0.5	98.76	98.61		
		1	99.45	98.98		
		2.5	99.65	100.00		
		5	99.38	100.00		
		10	99.42	100.00		
Cuckoo Rice Cooker	1	0.3	100.00	99.79	27.9	27.9
		0.5	100.00	99.75		
		1	100.00	99.80		
		2.5	100.00	100.00		
		5	100.00	100.00		
		10	100.00	100.00		
	2	0.3	100.00	98.89	33.0	30.5
		0.5	100.00	98.90		
		1	100.00	98.83		
		2.5	100.00	99.08		
		5	100.00	100.00		
		10	100.00	100.00		
	3	0.3	100.00	99.77	35.6	30.5
		0.5	100.00	99.89		
		1	100.00	99.96		
		2.5	100.00	99.92		
		5	100.00	99.72		
		10	100.00	97.44		
	4	0.3	99.52	97.16	30.5	33.0
		0.5	99.68	96.56		

		1	99.70	97.82		
		2.5	99.85	98.61		
		5	100.00	99.10		
		10	100.00	99.34		
	5	0.3	97.21	96.55	25.4	27.9
		0.5	98.79	99.36		
		1	97.34	99.39		
		2.5	96.33	100.00		
		5	100.00	100.00		
		10	100.00	100.00		
Sous Vide	1	0.3	99.90	97.73	38.1	30.5
		0.5	99.98	98.73		
		1	99.90	97.12		
		2.5	100.00	97.57		
		5	100.00	100.00		
		10	100.00	100.00		
	2	0.3	95.43	98.48	27.9	27.9
		0.5	97.37	99.84		
		1	97.93	99.82		
		2.5	98.89	98.91		
		5	99.46	100.00		
		10	99.39	100.00		
	3	0.3	99.49	98.33	27.9	27.9
		0.5	99.67	99.88		
		1	99.86	99.91		
		2.5	99.98	99.90		
		5	99.93	99.52		
		10	99.78	100.00		
	4	0.3	96.61	96.92	25.4	25.4
		0.5	97.71	97.62		
		1	97.78	96.85		
		2.5	97.30	97.22		
		5	100.00	99.21		
		10	100.00	100.00		
	5	0.3	100.00	98.79	30.5	27.9
		0.5	100.00	99.28		
		1	100.00	99.69		
		2.5	100.00	99.81		
		5	100.00	99.93		
		10	100.00	99.80		

Table S7. Filtration efficiency for control and treated Halyard Fluidshield 3 FFRs. None of the treatment methods tested reduces Halyard Fluidshield 3 FFR filtration performance below 95%. The pressure drop across N95 FFR was determined at a flow rate of 10 lpm.

Number of pinholes	Pressure Drop (mmH2O)	
	Across FFR Area 1	Across FFR Area 2
0	30.5	27.9
1	12.7	15.2
2	7.6	5.1
3	2.5	2.5

Table S8. Pressure drop across the N95 material for control and punctured Halyard Fluidshield 3 FFRs. The pressure drop across the N95 FFR material was determined at a flow rate of 10 lpm before and after one, two, and three punctures made with an 18-gauge needle.